Controlling Release Kinetics of Gentamicin from Silica Nano-carriers

by

Stefano Perni (PhD), Kerstin Martini-Gilching (BSc), Polina Prokopovich (PhD)

School of Pharmacy and Pharmaceutical Sciences, Cardiff University, Cardiff, UK

Corresponding author: Dr Polina Prokopovich

School of Pharmacy and Pharmaceutical Science

Cardiff University

Redwood Building, King Edward VII Avenue

Cardiff, UK

CF10 3NB

E-mail address: prokopovichp@cf.ac.uk

Abstract

Antibiotic release from a carrier can be employed to reduce the frequency of administration or prolong efficacy. In this work, we prepared silica nanoparticles loaded with gentamicin through different synthetis routes (entrapment, adsorption, covalent bonding and Layer-by-Layer (LbL) techniques). The nanocarriers physical-chemical properties were characterised and antibiotic release from the nanocarriers was monitored. The nanoparticles prepared entrapping gentamicin gave the highest drug load but completed the release over a period of 4 hours. No significant differences in antibiotic load were noticed between absorption or binding of gentamicin onto the silica nanoparticles surface; moreover the release of the drug occurred over 2 days. The nanoparticles coated with gentamicin through LbL technique released the antibiotic for 3 weeks. This work demonstrates that silica nanoparticles can be employed as antibiotic carriers providing a continuous release of antibiotic over a period that can be tuned through the choice of preparation method.

Keywords: Silica nanoparticles, gentamicin, LbL, antibiotic release

1 Introduction

Research on local delivery of antibiotic became more insistent as this approach would achieve high drug concentration where needed simultaneously avoiding the systemic side effects of antibiotics [1]; an additional benefit would be the reduction of antibiotic sub-lethal levels that are a known factor in the development of resistance towards these drugs [2]. These hypotheses have been experimentally confirmed as enhanced outcome have been reported when antibiotic delivery has been modulated through drug delivery systems [3]-[7].

Drug delivery systems for antibiotics can be prepared through the tethering of the molecule to a surface [8]-[10] or to a particle [11]-[14]. Alternatively, the drug can be encapsulated inside either nanoparticles [15] or liposomes [16]; another option is for the drug to be deposited onto a surface using Layer-by-layer (LbL) [17],[18].

Layer-by-layer is a self-assembly coating technique originally developed using polyelectrolytes of opposite charges alternately adsorbed onto a charged surface; after the deposition of each layer, the surface charge is reversed [19]. Moreover, uncharged materials like hydrophobic polymers can build up layers in LbL as formation forces are not limited to electrostatic interactions and almost every type of charged molecule or material can be used; examples are organic dyes, biological polysaccharides, polypeptides, DNA, proteins and antibiotics [20]. Also hydrophobic interactions, hydrogen bonding, charge transfer, covalent binding or biological recognition can supply the required attraction forces [20]. In addition to pharmaceutical applications, LbL method is often used in optical systems, sensors and biosensors, electronic devices and for surface protection [21]. Pharmaceutical research has employed LbL systems such as coating of particles [24], surfaces [25] and liposomes [26]; the coating of surfaces has been particular successful in prevent biofilm formation [27],[28]. Drugs can be added to the LbL system in different ways. The drug can be part of the coated layers (reservoir system) as one of the deposited layers instead of a polyelectrolyte or conjugated to one of the polyelectrolytes [28]; moreover the active molecule can be encapsulated

within the polyelectrolyte shell after core dissolution (matrix system) [24],[30]. LbL systems have been employed to prolong release [31], improve dissolution of hydrophobic drugs [33] and to improve cell targeting. The drug release profile can be influenced by the number of layers, the attraction forces between the different layers and the temperature [24]; whilst the release can triggered by pH [32], light [35] or sound [36].

Silica nanoparticles are well established drug carriers as they are extremely blood compatible [37]-[39] and their properties can be easily modified for the purpose of drug loading, controlled release and targeting characteristics [40]. Surface modification of nanoparticles can be performed in order to alter retention properties or to provide moieties for the further binding of active molecules [41]. The release profile, for example, is strongly influenced by loading capacity, surface properties and pore size of the nanoparticles [40].

Gentamicin is a large-spectrum antibiotic belonging to the aminoglycoside class; antibacterial activity is due to its ability to irreversibly bind ribosomes and halt proteins synthesis [42]. Gentamicin is employed to treat various infections such as topical, orthopeadic and ocular [43] and is used here as model antibiotic.

We hypothesised that silica nanoparticles loaded with antibiotics could be prepared through different synthetis routes resulting in different level of drug loading and different release kinetics. In this work, silica nanoparticles containing gentamicin have been prepared (1) entrapping the molecule inside the nanoparticles during synthesis; (2) adsorbing the antibiotic on the surface of nanoparticles either unfuctionalised or after surface functionalisation with amino or carboxyl groups; (3) covalently binding the drug molecule to amino or carboxyl functionalised nanoparticles and (4) coating the particles using the Layer-by-Layer technique (Figure 1). The chemical-physical properties of each type of nanoparticles have been determined and the release profiles established. Depending on the preparation method, the active release period can vary from a few hours to 3 weeks; therefore, fulfilling the requirements of different applications.

2 Experimental

2.1 Chemicals

Gentamicin sulphate, tetraethyl-orthosilicate (TEOS), 3-aminopropyltriethoxysilane (APTS), 2-(4-morpholino)-ethane sulfonic acid (MES), suberic acid bis-(N-hydroxy-succinimide ester), *ortho*-phthaldialdehyde reagent solution (OPA), sodium alginate (Mw 80.000-120.000 Da) and chitosan (Mw 190.000-310.000 Da) were purchased from Sigma-Aldrich. Triton X-100, ammonium hydroxide (29.6 %), cyclohexane, *n*-hexanol, Dichloromethane (DCM), isopropyl alcohol and methanol were purchased from Fisher Scientific. All chemicals were used as-received.

2.2 Synthesis silica-antibiotic nanocarriers

Silica nanoparticles (SiO_2) were prepared by hydrolysis of TEOS in reverse microemulsion. In a typical synthesis, 17.7 g of Triton X-100 were mixed with 16 ml of *n*-hexanol, 75 ml of cyclohexane and 4.8 ml of deionised water under vigorous stirring. Once the solution became transparent, 600 µl of ammonium hydroxide (29.6 %) were added. The solution was subsequently sealed and stirred for further 20 min, followed by addition of 1 ml of TEOS and stirring for 24 h. The SiO_2 nanoparticles were then recovered by adding ethanol (200 ml) to break the microemulsion and centrifuging at 3256 g for 10 min (LE-80K Ultracentrifuge, Beckman Coulter, UK) at 20 °C, the nanoparticles were then vigorously washed with methanol and DI water.

The silica nanoparticles surface were functionalized, when required, with amine groups adding 50 µl of APTS after 24 hours from the beginning of the synthesis to the microemulsion and incubating further 24 hours under stirring. The SiO_2-NH_2 nanoparticles were then recovered by adding ethanol (200 ml) to break the microemulsion and centrifuging at 3256 g for 10 min (LE-80K Ultracentrifuge, Beckman Coulter, UK) at 20 °C, the nanoparticles were then vigorously washed with methanol and DI water.

2.2.1 Entrapment of gentamicin into the silica nanocarriers

These nanoparticles were prepared as described above employing deionised water containing gentamicin sulphate (86 mg).

2.2.2 Succinylation silica nanocarriers

Amino functionalised nanoparticles (250 mg) and succinic anhydride (25 mg) were dispersed in DCM (100 ml). The suspension was purged with nitrogen and kept under vigorous stirring for 24 hours. DCM was evaporated under vacuum at room temperature. The succinylated nanoparticles (SiO_2-COOH) were washed three times with methanol and dried on a watch glass over night at room temperature.

2.2.3 Conjugation of gentamicin onto the silica nanocarriers

The conjugation of gentamicin to SiO_2-NH_2 nanoparticles was carried out as follows: 50 mg of antibiotic were dissolved in 100 ml of MES buffer (0.1 M, pH 6.0); this solution was used to disperse 250 mg of SiO_2-NH_2 and finally 5 mg of suberic acid bis-(N-hydroxysucciniimide ester) were added. The suspension was kept under vigorous mixing for 24 hours and then the conjugates were recovered centrifuging 3256 g for 10 min (LE-80K Ultracentrifuge, Beckman Coulter, UK) at 20 °C. The silica-antibiotic conjugates were washed three times in methanol and left to dry.

The conjugation of gentamicin to SiO_2-COOH nanoparticles was carried out as follows: Gentamicin sulphate (50 mg) was dissolved in 100 ml of MES buffer (0.1 M, pH 6). This solution was used to disperse succinylated nanoparticles (250 mg), 10 mg of N-hydroxysuccinimide (NHS) 10 mg of 1-(3-Dimethylaminopropyl)-3-ethyl-carbodiimide hydrochloride (EDC). The suspension was kept under vigorous stirring for 24 hours. The conjugates were recovered by centrifuging at 3256 g for 10 min (LE-80K Ultracentrifuge, Beckman Coulter, UK) at room temperature. After, the nanoparticles were washed three times with methanol. The nanoparticles were dried on a watch glass over night at room temperature.

2.2.4 Adsorption of gentamicin onto the silica nanocarriers

Gentamicin sulphate (50 mg) was dissolved in 100 ml of MES buffer (0.1 M, pH 6). This solution was used to disperse the different nanoparticles (250 mg). The suspension was kept under vigorous stirring for 24 hours. The adsorbed nanoparticles were recovered by centrifuging at 3256 g for 10 min (LE-80K Ultracentrifuge, Beckman Coulter, UK) at room temperature. Then the nanoparticles were washed three times with methanol and dried on a watch glass over night at room temperature.

2.2.5 Layer-by-layer deposition of gentamicin on silica nanocarriers

Dipping solutions were prepared in 100mM sodium acetate buffer pH = 5; alginate and chitosan were prepared at 2 mg/ml whilst gentamicin was prepared at 10 mg/ml.

About 250 mg of amino functionalised nanoparticles (SiO_2-NH_2) were dispersed in 25 ml of alginate solution and vortexed for 10 min. Particles were separated through centrifugation at 3256 g for 10 min. The supernatant was removed and the particles washed through redispersion in fresh acetate buffer pH = 5 and centrifuged at 3256 g for 10 min (LE-80K Ultracentrifuge, Beckman Coulter, UK). After discharging the supernatant, another layer was deposited dispersing the particles in gentamicin solution (25 ml) and vortexing for 10 min. The centrifugation/washing protocol was repeated and then again the particles were vortexed in alginate for 10 min. After repeating the centrifugation/washing protocol the particles were dispersed in chitosan for 10 min with vortexing. Finally, the particles were centrifuged, washed with clean buffer, deposited onto a glass watch and left to dry in a fume hood.

2.3 Silica-antibiotic nanocarriers characterisation

2.3.1 Transmission electron microscopy (TEM)

Size and shape of the conjugates was determined through transmission electron microscopy (TEM); 4 µl droplet of conjugates suspension were deposited on a plain carbon-coated copper TEM grid, water was evaporated under ambient laboratory conditions for several hours. Bright field TEM images were obtained using a TEM (Philips CM12, FEI Ltd, UK) operating at 80kV fitted with an X-ray microanalysis detector (EM-400 Detecting Unit, EDAX UK) utilising EDAX's Genesis software. Images (magnification of the images was x 100000) were recorded using a SIS MegaView III digital camera (SIS Analytical, Germany) and analysed with ImageJ; the diameter of at least 100 particles was determined for each type of nanoparticles.

2.3.2 Thermogravimetric analysis (TGA)

Thermogravimetric analysis (TGA) was performed using a Stanton Redcroft, STA-780; data were recorded from 25 to 600 °C with a constant heating rate of 10 °C min-1.

2.3.3 *Brunauer–Emmett–Teller* (BET)

Nitrogen adsorption-desorption isotherms were used to determine porosity and specific surface area of the silica nanoparticles. Isotherms at 77 K were obtained using BET Analyser, NOVA-e™ Series (Quantochrome Instruments, USA). Before starting the adsorption measurements, all silica samples were degassed under vacuum at 80° C for 4 h. The BET surface was calculated through the MultiPoint BET model using the instrument software. The total pore volume was determined for pores with a radius less than 405 Å at P/Po = 0.97 by the instrument software.

2.3.4 Zeta potential

Approximately 2 mg sample were dispersed in 1 ml of buffer solution at the chosen pH. The suspension was vortexed and transferred to a capillary cell. The zeta potential was measured immediately using Zetasizer ZEN 3600, Nano Series (Malvern, UK). For pH = 4 and 5, an acetic buffers (0.1 M) were prepared, whereas phosphate buffer (0.1 M) was employed for pH = 7. The highest pH value was achieved with a glycine buffer pH = 9 (0.1 M).

2.4 Gentamicin release

Gentamicin release was quantified dispersing conjugates (5 mg) in 1 ml of NaH_2PO_4 - Na_2HPO_4 buffer at pH = 7.4 and 5; the suspensions were kept in eppendorf and incubated at 37 °C. At prefixed times, samples were centrifuged and the supernatant collected for antibiotic quantification, the particles were resuspended in 1 ml of the corresponding buffer and incubated at 37 °C.

Gentamicin was quantified thorough fluorescence spectroscopy using *o*-phthaldialdehyde (OPA); 100 µl of buffer containing antibiotic were mixed with 100 µl of *iso*-propanol and 100 µl of OPA reagent; after 30 min at room temperature in the dark, 200 µl of the mixture were transferred in a black 96 wells plate and the fluorescence determined (excitation wavelength = 340 nm and emission wavelength = 450 nm) with a fluoroscan (FLUOROstar Optina, BMG Labtech); standards of known gentamicin concentration were also analysed simultaneously to provide calibration.

All characterisations were carried out on nanoparticles obtained from at least three independent batches; results are presented as mean ± standard deviation.

3 Results

The silica nanoparticles unconjugated (SiO_2) appeared spherically shaped (Figure 2) with a narrowly distributed diameter. The particles diameters population distribution was closely modelled by a Gaussian model with a mean of 55.5 nm and a standard deviation of 6.6 nm. Surface functionalisation, gentamicin conjugation or absorption along with LbL deposition did not have effect on these parameters (data not shown).

Examples of adsorption and desorption curves of nitrogen on the nanocarriers are presented in Figure 3 were differences between unfunctionalised nanoparticles and nanocarriers with entrapped

gentamicin are evident. The BET parameters are summarised in Table 1 and revealed that the pore size of the particles was affected only by the entrapment of gentamicin. The functionalisation also resulted in a reduced BET surface area but further conjugation/adsorption did not affect either surface area or pores size of the nanocarriers.

During TGA analysis (Figure 4) all particles exhibited a weight loss of about 8-10% in the temperature range 20-100 °C; with increasing temperature the weight loss of the samples increased monotonically reaching a plateau after about 600°C. Unfunctionalised and unloaded nanoparticles (SiO_2) returned a weight loss of 14%. this was the lowest of all samples (Table 1), whilst the nanocarriers with entrapped gentamicin had the greatest weight loss (31%). Nanoparticles loaded with gentamicin had the same mass loss regardless of the fact that the antibiotic was either conjugated or adsorbed; for both silica functionalised with amino groups (SiO_2-NH_2) or with carboxyl groups (SiO_2-COOH), the weight loss increased when the nanocarriers were loaded with gentamicin, from 17 to 19 %.

The zeta potentials of the silica nanoparticles at pH values ranging from 4 to 9 are shown in Figure 5; in all cases the zeta potential decreased with increasing pH. Unfunctionalised nanocarriers had a negative charge throughout the pH range tested regardless of the presence of adsorbed gentamicin. Particles with entrapped antibiotic exhibited a slightly higher zeta potential than the corresponding unloaded nanocarriers. Amino functionalised silica nanoparticles had a remarkably high positive zeta potential (about +40 mV) at pH = 4 and 5; this decreased towards neutrality when pH increased to 7 and 9. The presence of gentamicin decreased the zeta potential compared to the unloaded particles with not significant differences between adsorbed or conjugated antibiotic at all pHs tested but 9. Silica nanoparticles functionalised with carboxyl acid groups had a positive zeta potential at pH = 4 while at more alkaline pH values the zeta potential was negative. The conjugation or adsorption of gentamicin resulted in higher zeta potential values through the pH range tested.

The percentage of gentamicin released from the nanocarriers over time in buffer at pH = 5 and 7.4 is shown in (Figure 6). When gentamicin was entrapped in the silica nanoparticles, not all the antibiotic was able to leave and the release occurred in the first 4 hours, the maximum amount of gentamicin was higher at pH = 5 than at pH = 7.4. Unfunctionalised nanoparticles with adsorbed gentamicin released very little antibiotic in the first few hours and no more after this regardless of the pH tested. Functionalised silica nanoparticles both with amino and carboxyl groups exhibited a sustained release of antibiotic for at least 2 days. No significant difference was found between adsorption and conjugation method of loading gentamicin onto the nanocarriers. The kinetic of release was quicker at pH = 7.4 than at pH = 5.

During LbL deposition the organic content of the nanocarriers increased after each layer as shown by the TGA thermograms (Figure 7a), additionally the surface charge initially positive became negative after the deposition of the alginate layers and positive after the deposition of chitosan (Figure 7b). After the deposition of gentamicin the surface charge was mildly positive. The release of antibiotics from silica nanocarriers prepared through LbL continued for 3 weeks and was affected by the pH of the solution (Figure 7b).

4 Discussion

The Stöber synthetic method for silica nanoparticles is based on the hydrolysis of TEOS (soluble in water) in an water in oil emulsion; because of the nanoparticles growth occurs inside the water droplet, the final size and shape of synthesised nanoparticles depends on the size and shape of water droplets [44]. The variation of the organic solvent and of the other reaction conditions has been successfully employed to prepare silica nanoparticles in a wide range of sizes. Our results (Figure 2) are consistent with other works employing the same reagents and conditions [48]; furthermore the limited number of polyelectrolytes layers deposited onto the nanocarriers during LbL was no sufficient to increase the average particle diameter. Because of the mechanism of synthesis of the

nanoparticles, entrapment of the antibiotic had no effect on size of the nanocarriers; however when gentamicin was present in the water phase, the growth of the silica particles was disturbed by the antibiotic resulting in nanoparticles with higher surface area (Table 1 and Figure 3). The adsorption-desorption curves of N_2 (Figure 3) depict a typical Type II profile confirming the lack of mesopores in the nanocarriers. Furthermore, the lower amount of N_2-adsorbed/desorbed by the nanocarriers with entrapped gentamicin compared to the other carriers, along with the lower values of total pore volume, suggests that the antibiotic is entangled inside the network of silane-oxygen bonds as suggested by Capeletti et al. [15] and Hakeem et al. [49]. Moreover, as gentamicin partitions predominately in the aqueous phase, the nanocarriers prepared through this protocol had the highest load of antibiotic. Similar loading results were reported for the encapsulation of vancomycin in mesoporous silica nanoparticles [15]. The functionalisation of the nanoparticles, the adsorption or conjugation of the antibiotic or the LbL deposition are processes affecting only the outer surface of the nanoparticles thus they did not impact the overall size and shape of the carriers. Likewise, these processes were also unable to impact the porosity of the nanoparticles, on the contrary they reduced the surface area of the nanocarriers available for gas adsorption as seen in the BET analysis (Table 1 and Figure 3); this was in consequence of the presence of the antibiotic on the surface that reduced the active sites for gas adsorption.

TGA is routinely employed to quantify the organic and inorganic fraction of substrates. At temperatures below 100 °C (Figure 4) the weight loss shown by the samples is related to water adsorbed, at higher temperatures the weight loss depends on the organic fraction presents on the nanoparticles. The unfunctionalised nanoparticles exhibited almost no organic fraction; this was expected as only silane and oxygen were present in this samples. Whereas both the amino and carboxyl acid functionalised carriers presented weight loss greater than unfuctionalised particles in virtue of either the amino propyl-silane used to coat the surface of the bare silica nanoparticles or the subsequent succinylation. The higher weight losses exhibited by the samples with gentamicin are consistent with the successful load of the carriers with the antibiotic. The loading protocols

through adsorption or conjugation, returned similar weight losses; hence the efficiency of the two approaches was comparable.

The charge exhibited by the particles, and expressed through the zeta potential, depends on the balance between the protonated and the unprotonated groups present on the surface. Such balance is influenced by the pH of the solution; for example, amino groups are positively charged at low pHs values because of the protonation of the nitrogens while they are neutral at high pHs. On the other hand, carboxyl groups are negatively charged at high pHs in virtue of the protonation of the hydroxyl groups at low pHs. The pH resulting in half of the groups protonation (and half of the groups deprotonation) corresponds to the value of pKa of the dissociation reaction (Henderson - Hasslbach equation). Cells are generally negatively charged hence strong electrostatic interactions would be originated towards positively charged particles, however surfaces appendices present on cell can overcome the possible repulsive barrier observed when facing negatively charged surfaces; evidence has shown that positively nanoparticles have higher toxicity than negatively charged ones [45]. Human body pH is generally close to neutral, however there are some fluids that exhibit extreme acidity (stomach is about pH = 3.5 [46]) or alkalinity (pancreatic fluid is about pH = 8.8 [47]) therefore the pH range employed for our studies covers such spectrum. Unfunctionalised particles exhibit hydroxyl groups on the surface that behave as weak acid; hence they are protonated and nearly neutral at pH values up to about 7, while they are deprotonated, and with negative charge, in alkaline solutions. Amino groups are known to be protonated at alkaline pHs, while carboxylic acids are known to be protonated at pHs lower than 4-5 as the pKa of these compounds is about 4.5. Adsorption and conjugation of gentamicin was expected to reduce the number of carboxyl groups on the surface of the carriers available for dissociation thus reducing the number of negative charges; analogously for amino groups the conjugation or adsorption of antibiotic would interfere with the ability of the nitrogen to be protonated and such reducing the number of positive charges on the surface of the carriers. The pH dependence of the nanoparticles (Figure 5) followed

very well this description, providing further confirmation of the presence of either the desired groups or the antibiotic on the surface of the carriers.

Two different pH buffers were employed to study the release of gentamicin from the nanocarriers to mimic two distinct situations: prevention of infection represented by physiological (pH = 7.4) conditions and treatment of established infections represented by acid conditions (pH = 5) [50]-[52]. The release of gentamicin when entrapped into silica nanoparticles is not controlled as all the antibiotic that could be freed is released in the first hours of contact with aqueous solutions (Figure 6); this is the consequence of the porosity of the nanocarriers that leads to water uptake. On the contrary, when gentamicin was adsorbed on unfunctionalised particles very little release was observed; at pH = 5 a greater amount of antibiotic was released from the particles than for pH = 7.4 indicating that the adsorption of gentamicin is more stable in neutral conditions. Interestingly, not all antibiotic loaded in the particles through entrapment could be released from the nanocarriers, this could have been caused by the ability of the antibiotic molecules to migrate through a limited distance inside the particles resulting in only the molecules present on the outer layers to be released. This is the mechanism hypothesised to explain why only about 10% of gentamicin mixed in bone cement is released over time [53]. However, because of the limited thickness of the particles compared to bone cement this justification seem unlikely; alternatively it can be hypothesised some of antibiotic loaded through entrapment is effectively adsorbed on the surface of the silica nanoparticles and our results show that desorption from these carriers is difficult. Furthermore, in all cases not all the antibiotic initial present on the silica nanoparticles was released (Figure 6), even though not to the same extent as for the entrapped route; this seems to suggest that a certain amount of gentamicin can irreversibly bind to the silica surface. The higher adsorption of gentamicin onto silica at pH = 7.4 could also explain the lower total amount of antibiotic released from particles with entrapped antibiotic in this condition than in acidic environment.

Functionalised particles appeared more suitable for providing antibiotic release for at least few days, remarkably no difference was noticed between conjugation of the antibiotic or its adsorption.

Because the release from conjugated nanocarriers requires the hydrolysis of ester bonds, we expected that the kinetic of gentamicin release to be slower compared to the adsorption. Similar kinetic of release were reported from gentamicin conjugated onto the surface of functionalised gold nanoparticles through the formation of ester bonds [12]; this points towards the controlling role of the type of bond on the release kinetic of conjugated antibiotic on surfaces. The functionalisation of the particles had an extreme impact on the loading and desorption of gentamicin, when either amino (positively charged) or carboxyl (negatively charged) were present on the surface more antibiotic was adsorbed onto the surface and the release of gentamicin was almost complete compared to about 10% seen in unfunctionalised silica nanoparticles. Gentamicin is charged as it exhibit amino and hydroxyl groups; the adsorption was carried out at pH = 6 were the functionalised nanoparticles possessed surface charges facilitating the electrostatic interaction between particles and antibiotic enhancing the amount of drug adsorbed compared to unfunctionalised molecules.

In this work, amino functionalised silica nanoparticles provided a positively charged substrate and we exploited the positive charge exhibited by gentamicin at physiological conditions, in virtue of the amino groups present on the molecule, to sandwich the antibiotic between alginate layers that are negatively charged. The choice of the polyelectrolytes used in this work (chitosan and alginate) was driven by the high biocompatibility of these biomacromolecules compared to other polyelectrolytes that are sometimes used for LbL i.e. poly(styrene sulfonate), poly(allylamine hydrochloride [54] and poly(diallyldimethyl ammonium chloride) [55].

Drug release from LbL coating can occur either through diffusion of the molecule across the polyelectrolytes layers or as result of deposited layers erosion [56], so called “delamination”. These two mechanisms also control the shape of the release profile; if LbL erosion is governing the release, then the cumulative amount of drug unbound increases linearly over time until a plateau is reached, corresponding to full LbL consumption. When diffusion of the drug through the layers is the controlling mechanism, the cumulative amount of drug follows a Fickian profile instead [56]. The release profile from our silica nanocarriers loaded through LbL (Figure 7c) depicts a

mechanism controlled by drug diffusion, this mechanism is also the likely reason for the similar release kinetics at pH = 5 and pH = 7.4 as the acidity of the solution does not influence the diffusion of the drug through the deposited polyelectrolytes layers. Furthermore, the need to cross the different deposited layers results in the prolonged release of gentamicin compared to the other nanocarriers prepared in this work where the antibiotic is freely available.

We have shown that silica nanocarriers loaded with gentamicin can be prepared through various protocols; depending on the preparation route, release of the drug can be tailored to different applications. For example, the complete release of the antibiotic in a few days appears suited for the treatment of local infections as it would allow the reduction of medications and thus improving patient compliance. On the other end, gentamicin release for many weeks is well suited for orthopaedic applications, such as encapsulation in bone cement. Because of the general nature of the phenomena employed in the preparation of our silica gentamicin nanocarriers (i.e. electrostatic forces and conjugation), it is easily foreseeable how the silica nanocarriers could be employed for the controlled delivery of other molecules.

Other types of antibiotic releasing silica nanoparticles have been proposed, however in some no attempt was made to determine the effective period of time that the drug was release [57],[58], whilst in others only one preparation protocol was presented hence the role of the protocol of synthesis in charactering the release was not established [59].

It is well known that the current mixing of antibiotics in bone cement is released only for the first few days after surgery [60], while infections can occur at the site even months after implantation [61]. Recently, antibiotics have been bound to silica nanocarriers either through conjugation [62] or co-precipitation [58] in order to provide controlled release. Despite the excellent blood compatibility and low toxicity demonstrated by these nanocarriers [62], the release was sustained for about 1 week; hence not as effective as the nanocarriers presented in this work. LbL has also been used to prepare antibiotic loaded silica nanocarriers [63],[64]. This approach was employed to

entrap the drug under polyelectrolytes that enhance bacterial cell penetration [64] or to seal the drug inside mesoporous particles and, therefore, the polyelectrolytes acted as "gatekeeper" [49]; in this way sustained the release for about 10 days was achieved [63]; again not as effective as the nanocarriers presented in this work.

Mesoporous silica nanoparticles (MSN) have been widely investigated as drug delivery vehicles [65]-[69] with their main benefit compared to nonporous nanoparticles being the higher surface available for drug loading. When surface conjugation or adsorption is carried out, the drug release kinetics is unlikely to depend on the presence of pores and the conclusions of our study can be translated to mesoporous silica nanoparticles. When LbL is utilised as gatekeeping the released is delayed, instead of sustained, as the drug entrapped in the pores has to cross the layers in order to become available. As shown by Tamanna et al. [63] with increasing number of polyelectrolytes layers the concentration of antibiotic release tend to present a lag phase.

Nanocarriers based drug delivery systems for antibiotics require varying release kinetic according to the application they are design to fulfil; the desired release period can be from few days to weeks. We have shown the versatility of silica nanoparticles to be prepared as antibiotic delivery system and correlated the preparation protocol to the chosen release kinetics specification.

5 Acknowledgements

This publication was supported by the Life Science Research Network Wales, an initiative funded through the Welsh Government's Ser Cymru program (project 507444).

6 References

[1] Gao P., Xin Nie, Meijuan Zou, Yijie Shi, Gang Cheng. Recent advances in materials for extended-release antibiotic delivery system. The Journal of Antibiotics 2011; 64:625-634

[2] Turnidge J.D. The pharmacodynamics of beta-lactams. Clin. Infect. Dis. 1998;27:10-22.

[3] Blasi F., Aliberti S., Tarsia P. Clinical applications of azithromycin microspheres in respiratory tract infections. Int. J. Nanomedicine 2007;2:551-559

[4] Roberts J.A., Lipman J., Blot S., Rello J. Better outcomes through continuous infusion of time-dependent antibiotics to critically ill patients? Curr. Opin. Crit. Care 2008;14:390-396.

[5] Roberts J.A., Paratz J., Paratz E., Krueger W.A., Lipman, J. Continuous infusion of beta-lactam antibiotics in severe infections: a review of its role. Int. J. Antimicrob. Agents 2007;30:11-18

[6] Moriyama B., Henning S.A., Neuhauser M.M., Danner R.L., Walsh T.J. Continuous-infusion beta-lactam antibiotics during continuous venovenous hemofiltration for the treatment of resistant gram-negative bacteria. Ann. Pharmacother. 2009;43:1324-1337.

[7] Talan D.A., Naber K.G., Palou J., Elkharrat D. Extended-release ciprofloxacin (Cipro XR) for treatment of urinary tract infections. Int. J. Antimicrob. Agents 2004;(23 Suppl 1):S54-66.

[8] Hickok N.J., Shapiro I.M. Immobilized antibiotics to prevent orthopedic implant infections. Adv Drug Deliv Rev. 2012;64(12):1165-1176.

[9] Monteiro N., Martins M., Martins A., Fonseca N.A., Moreira J.N., Reis R.L., Neves N.M. Antibacterial activity of chitosan nanofiber meshes with liposomes immobilized releasing gentamicin. Acta Biomater. 2015;18:196-205

[10] Goissis G., Sousa M.H. Characterization and in vitro release studies of tetracycline and rolitetracycline immobilized on anionic collagen membranes. Mat. Res. 2009;12(1):69-74

[11] Ahangari A., Salouti M., Heidari Z., Kazemizadeh A.R., Safari A.A. Development of gentamicin-gold nanospheres for antimicrobial drug delivery to Staphylococcal infected foci. Drug Deliv. 2013;20(1):34-39

[12] Perni S., P. Prokopovich P. Continuous Release of Gentamicin from Gold Nanocarriers" RSC Advances 2014;4:51904-51910

[13] Motamedi H., Mazdeh S.K., Azim A.K., Mehrabi M.R. Optimization of Gold Nanoparticle Biosynthesis by Escherichia coli DH5[alpha] and its Conjugation with Gentamicin. J Nano Res 2015;32:93-105

[14] Salouti M., Heidari Z., Ahangari A., Zare S. Enhanced delivery of gentamicin to infection foci due to *Staphylococcus aureus* using gold nanorods. Drug Deliv. 2016;23(1):49-54

[15] Capeletti L.B., de Oliveira L.F., Gonçalves K. de A., de Oliveira J.F., Saito Â., Kobarg J., dos Santos J.H., Cardoso M.B. Tailored silica-antibiotic nanoparticles: overcoming bacterial resistance with low cytotoxicity. Langmuir. 2014;;30(25):7456-7464

[16] Mugabe C., Azghani A.O., Omri A. Liposome-mediated gentamicin delivery: development and activity against resistant strains of Pseudomonas aeruginosa isolated from cystic fibrosis patients. J. Antimicrob. Chemother. 2005;55(2):269-671

[17] Chuang H.F., Smith R.C., Hammond P. T. Polyelectrolyte multilayers for tunable release of antibiotics. Biomacromolecules 2008;9:1660-1668.

[18] Moskowitz J.S., Blaisse M.R., Samuel R.E., Hsu H.P., Harris M.B., Martin S.D., Lee J.C., Spector M., Hammond P.T. The effectiveness of the controlled release of gentamicin from polyelectrolyte multilayers in the treatment of *Staphylococcus aureus* infection in a rabbit bone model. Biomaterials. 2010;31(23):6019-6030

[19] Lu Z., Eadula S., Zheng Z., Xu K., Grozdits G., Lvov Y. Layer-by-layer nanoparticle coatings on lignocellulose wood microfibers. Colloids and Surfaces A: Physicochemical and Engineering Aspects 2007; 292 (1):56-62

[20] Tang Z., Wang Y., Podsiadlo P., Kotov N. Biomedical Applications of Layer-by-Layer Assembly: From Biomimetics to Tissue Engineering. Advanced Materials 2006;18(24):3203-3224

[21] Decher G., Hong J.D., Schmitt J. Buildup Of Ultrathin Multilayer Films by a Self-Assembly Process .3. Consecutively Alternating Adsorption of Anionic and Cationic Polyelectrolytes on Charged Surfaces. Thin Solid Films 1992;210(1-2):831-835

[22] Richardson, J.J.; Björnmalm, M.; Caruso, F. Multilayer assembly. Technology-driven layer-by-layer assembly of nanofilms. Science 2015, 348, aaa2491

[23] Amanchukwu C.V., Gauthier M., Batcho T. P., Symister C.,. Shao-Horn Y, D'Arcy J. M., Hammond P. T. Evaluation and Stability of PEDOT Polymer Electrodes for Li–O2 Batteries. J Phys Chem Let 2016;7: 3770

[24] Zhou J., Pishko M., Lutkenhaus J. Thermoresponsive Layer-by-Layer Assemblies for Nanoparticle-Based Drug Delivery. Langmuir 2014;30(20):5903-5910

[25] Hsu B.B., Hagerman S.R., Hammond P.T. Rapid and efficient sprayed multilayer films for controlled drug delivery. Journal of applied polymer science 2016;133(25)

[26] Yoo C.Y., Seong J.S., Park S.N. Preparation of novel capsosome with liposomal core by layer-by-Layer self-assembly of sodium hyaluronate and chitosan. Colloids and surfaces B 2016;44:99-107

[27] Kruk T., Szczepanowicz K., Kręgiel D., Szyk-Warszyńska L., Warszyński P. Nanostructured multilayer polyelectrolyte films with silver nanoparticles as antibacterial coatings. Colloids Surf B Biointerfaces. 2016;137:158-166

[28] Kovačević D., Pratnekar R.,, Torkar K.G., Salopek J., Dražić G., Abram A., Bohinc K. Influence of Polyelectrolyte Multilayer Properties on Bacterial Adhesion Capacity Polymers 2016;8(10):345

[29] Authimoolam S.P, Puleo D.A., Dziubla T.D. Affinity based multilayered polymeric self-assemblies for oral wound applications. Advanced healthcare materials 2013;2(7):983-992

[30] Reibetanz U., Claus C., Typlt E., Hofmann J., Donath E. Defoliation and Plasmid Delivery with Layer-by-Layer Coated Colloids. Macromolecular Bioscience 2006; 6(2):153-160

[31] Luo D., Shahid S., Wilson R.M., Cattell M.J., Sukhorukov G.B. Novel Formulation of Chlorhexidine Spheres and Sustained Release with Multilayered Encapsulation. ACS applied materials & interfaces 2016;8(20):12652-12660

[32] Yilmaz M.D. Layer-by-layer hyaluronic acid/chitosan polyelectrolyte coated mesoporous silica nanoparticles as pH-responsive nanocontainers for optical bleaching of cellulose fabrics. Carbohydrate polymers 2016;146:174-180

[33] Kola-Mustapha A.T., Armitage D., Abioye A.O. Development of aqueous ternary nanomatrix films: A novel 'green' strategy for the delivery of poorly soluble drugs. International journal of pharmaceutics 2016;515(1-2):616-631

[34] Reibetanz A., Hübner D., Jung M., Liebert U.G., Claus C. Influence of Growth Characteristics of Induced Pluripotent Stem Cells on Their Uptake Efficiency for Layer-by-Layer Microcarriers. ACS nano 2016;10(7):6563-6573

[35] Bao C.Y., Ma B.H., Liu J.L., Wu Z.N., Zhang H., Jiang Y.J., Sun J.Q. Near-Infrared Light-Stimulus-Responsive Film as a Sacrificial Layer for the Preparation of Free-Standing Films. Langmuir 2016;32(14):3393-3399

[36] Zhang Z.X., Tang Z.F., Liu W.P., Zhang H.X., Lu Y., Wang Y.Y., Pang W., Zhang H., Duan X,X, Acoustically Triggered Disassembly of Multilayered Polyelectrolyte Thin Films through Gigahertz Resonators for Controlled Drug Release Applications. Micromachines 2016;7(11):194

[37] Ngamcherdtrakul W., Morry J., Gu S., Castro D.J., Goodyear S.M., Sangvanich T., Reda M.M., Lee R., Mihelic S.A., Beckman B.L., Hu Z., Gray J.W., Yantasee W. Cationic Polymer Modified Mesoporous Silica Nanoparticles for Targeted SiRNA Delivery to HER2+ Breast Cancer. Adv. Funct. Mater. 2015;25(18):2646-2659

[38] He Q.J., Shi J.L. Mesoporous silica nanoparticle based nano drug delivery systems: synthesis, controlled drug release and delivery, pharmacokinetics and biocompatibility. J. Mater. Chem. 2011;21(16):5845-5855

[39] Yildirim A., Ozgur E., Bayindir M. Impact of mesoporous silica nanoparticle surface functionality on hemolytic activity, thrombogenicity and non-specific protein adsorption. J. Mater. Chem. B 2013;1(14):1909-1920

[40] He Q., Shi J. Mesoporous silica nanoparticle based nano drug delivery systems: synthesis, controlled drug release and delivery, pharmacokinetics and biocompatibility. Journal of Materials Chemistry 2011; 21(16): 5845-5855.

[41] Das D., Yang Y., Brien J., Breznan D., Nimesh S., Bernatchez S., Hill M., Sayari A., Vincent R., Kumarathasan P. Synthesis and Physicochemical Characterization of Mesoporous Nanoparticles. Journal of Nanomaterials 2014;2014 Article ID 176015.

[42] Tangy F., Moukkadem M., Vindimian E., Capmau M.L., Le Goffic F. Mechanism of action of gentamicin components. Characteristics of their binding to Escherichia coli ribosomes. Eur J Biochem. 1985;147(2):381-386

[43] Mascaretti O.A. Bacteria versus antimicrobial agents – An integrated approach. American Society Microbiology Press 2003

[44] Wang X.D., Dong Z.X., Sang T., Cheng X.B., Li M.F., Chen L.Y., Wang Z.S. Preparation of spherical silica particles by Stöber process with high concentration of tetra-ethyl-orthosilicate. J Colloid Interface Sci. 2010;;341(1):23-29

[45] Suresh A.K., Pelletier D.A., Wang W., Morrell-Falvey J.L., Gu B., Doktycz M.J. Cytotoxicity induced by engineered silver nanocrystallites is dependent on surface coatings and cell types. Langmuir 2012;28(5):2727-2735

[46] Miederer S.E., Grübel P. Profound increase of *Helicobacter pylori* urease activity in gastric antral mucosa at low pH. Dig. Dis. Sci. 1996;41(5):944-949

[47] Takeshima T., Adler M., Nacchiero M., Rudick J., Dreiling D.A. Effects of duodenal alkalinization on pancreatic secretion. Am. J. Gastroenterol. 1977;67(1):54-62

[48] Guo Y., Rogelj S., Zhang P. Rose Bengal-decorated silica nanoparticles as photosensitizers for inactivation of gram-positive bacteria. Nanotechnology. 2010;21(6):065102

[49] Hakeem A., Duan R., Zahid F., Dong C., Wang B., Hong F., Ou X., Jia Y., Lou X., Xia F. Dual stimuli-responsive nano-vehicles for controlled drug delivery: mesoporous silica nanoparticles end-capped with natural chitosan. Chem. Commun. 2014;50:13268-13271

[50] Kinnari T.J., Esteban J., Martin-de-Hijas N.Z., Sánchez-Muñoz O., Sánchez-Salcedo S., Colilla M., Vallet-Regí M., Gomez-Barrena E. Influence of surface porosity and pH on bacterial adherence to hydroxyapatite and biphasic calcium phosphate bioceramics. J Med Microbiol. 2009;58:132-137

[51] Ribeiro M., Monteiro F.J., Ferraz M.P. Infection of orthopedic implants with emphasis on bacterial adhesion process and techniques used in studying bacterial-material interactions. Biomatter 2013;2(4),176-194

[52] Simmen HP, Battaglia H, Kossmann T, Blaser J. Effect of peritoneal fluid pH on outcome of aminoglycoside treatment of intraabdominal infections. World J Surg 1993;17:393-397

[53] Shen S.C., Ng W.K., Dong Y.C., Ng J., Tan R.B.H. Nanostructured material formulated acrylic bone cements with enhanced drug release. Mater. Sci. Eng. C 2016;58:233-241

[54] Decher G. Fuzzy Nanoassemblies: Toward Layered Polymeric Multicomposites. Science 1997;29:1232–1237

[55] Clark S.L., Montague M.F., Hammond P.T. Ionic Effects of Sodium Chloride on the Templated Deposition of Polyelectrolytes Using Layer-by-Layer Ionic Assembly. Macromolecules 1997;30:7237-7244

[56] Smith R.C., Riollano M., Leung A., Hammond P.T. Layer-by-layer platform technology for small-molecule delivery. Angew Chem Int Ed Engl. 2009;48(47):8974-8977

[57] Balaure P.C., Popa R.A., Grumezescu A.M., Voicu G., Rădulescu M., Mogoantă L., Bălşeanue T.A., Mogoşanu G.D. Biocompatible hybrid silica nanobiocomposites for the efficient delivery of anti-staphylococcal drugs. International Journal of Pharmaceutics. 2016;510(2):532-542

[58] Mosselhy D.A., Ge Y., Gasik M., Nordström K., Natri O., Hannula S.P. Silica-gentamicin nanohybrids: Synthesis and antimicrobial action. Materials. 2016;9(3):170

[59] Tamanna T., Bulitta J.B., Landersdorfer C.B., Cashin V., Yu A. Stability and controlled antibiotic release from thin films embedded with antibiotic loaded mesoporous silica nanoparticles. RSC Advances. 2015;5(130):107839-107846

[60] Bridgens J., Davies S., Tilley L., Norman P., Stockley I. Orthopaedic bone cement: do we know what we are using? J Bone Joint Surg Br. 2008;90(5):643-647.

[61] Anagnostakos K., Schmid N.V., Kelm J., Grün U., Jung J. Classification of hip joint infections. Int J Med Sci. 2009; 6(5): 227-233.

[62] Agnihotri S., Pathak R., Jha D., Roy I., Gautam H.K., Sharmaa A.K., Kumar P. Synthesis and antimicrobial activity of aminoglycoside-conjugated silica nanoparticles against clinical and resistant bacteria. New J. Chem. 2015;39:6746-6755

[63] Tamanna T., Bulitta J.B., Yu A. Controlling antibiotic release from mesoporous silica nano drug carriers via self-assembled polyelectrolyte coating. J Mater Sci Mater Med. 2015;26(2):117

[64] Wu Y., Long Y., Li Q.L., Han S., Ma J., Yang Y.W., Gao H. Layer-by-Layer (LBL) Self-Assembled Biohybrid Nanomaterials for Efficient Antibacterial Applications. ACS Appl Mater Interfaces. 2015;7(31):17255-17263

[65] Rosenholm J. M., Sahlgren C., Lindén M. Multifunctional mesoporous silica nanoparticles for combined therapeutic, diagnostic and targeted action in cancer treatment. Current Drug Targets 2011;12(8):1166-1186

[66] Li Z., Barnes J.C., Bosoy A., Stoddart J.F., Zink J.I. Mesoporous silica nanoparticles in biomedical applications. Chemical Society Reviews 2012;41(7): 2590-2605

[67] Wu S.H., Mou C. Y., Lin H.P. Synthesis of mesoporous silica nanoparticles. Chemical Society Reviews 2013;42(9):3862-3875

[68] Yamada H., Urata C., Ujiie H., Yamauchi Y., Kuroda K. Preparation of aqueous colloidal mesostructured and mesoporous silica nanoparticles with controlled particle size in a very wide range from 20 nm to 700 nm. Nanoscale 2013;5(13): 6145-6153

[69] Yang P., Gai S., Lin, J. Functionalized mesoporous silica materials for controlled drug delivery. Chemical Society Reviews 2012;41(9):3679-3698.

Table 1. BET parameters and TGA total mass loss for different Si nanocarriers prepared.

Sample	BET surface area [m^2/g]	Total pore volume [cm^3/g]	TGA Mass loss (%)
SiO_2	65 ± 5	0.32 ± 0.04	14 ± 2
SiO_2 GS entrapped	78 ± 6	0.18 ± 0.03	31 ± 4
SiO_2 GS adsorbed	45 ± 4	0.35 ± 0.03	15 ± 2
SiO_2-NH_2	48 ± 3	0.27 ± 0.05	17 ± 3
SiO_2-NH_2 GS conjugated	48 ± 5	0.36 ± 0.03	19 ± 3
SiO_2-NH_2 GS adsorbed	42 ± 7	0.32 ± 0.07	19 ± 4
SiO_2-COOH	41 ± 3	0.36 ± 0.05	17 ± 4
SiO_2-COOH GS conjugated	47 ± 6	0.31 ± 0.05	19 ± 3
SiO_2-COOH GS adsorbed	46 ± 4	0.44 ± 0.06	19 ± 4

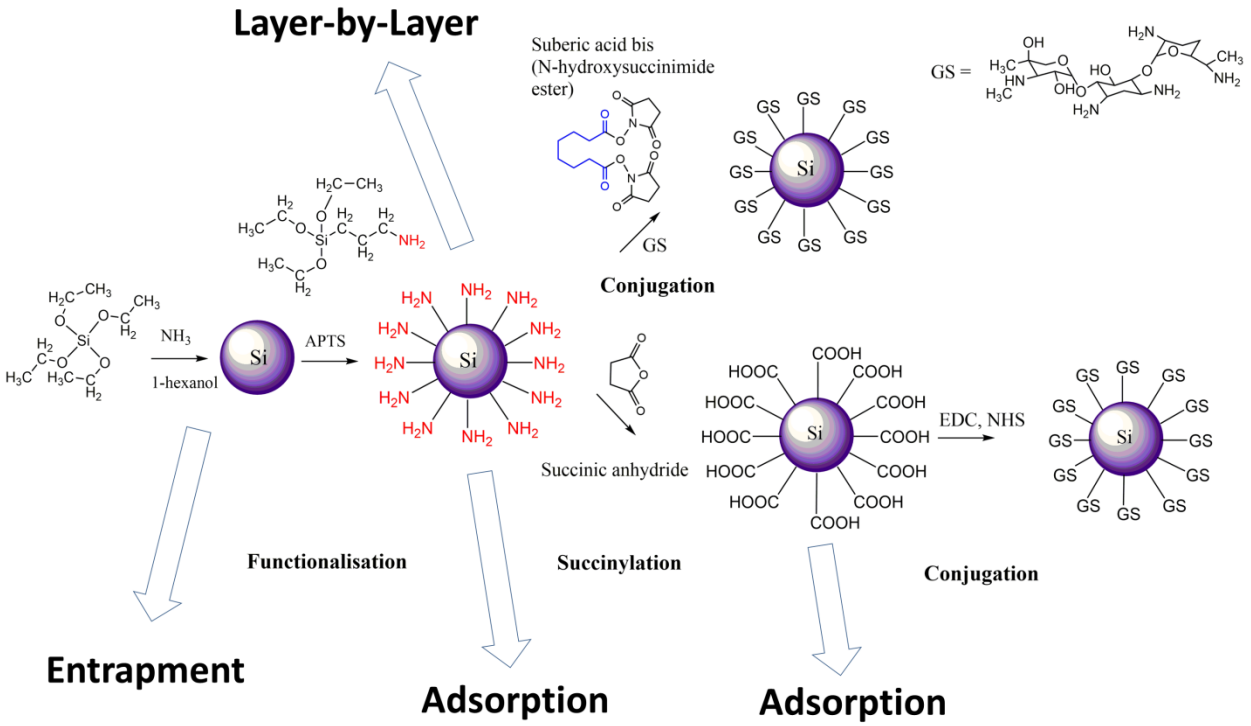

Figure 1. Reactions scheme involved in the nanocarriers preparation routes.

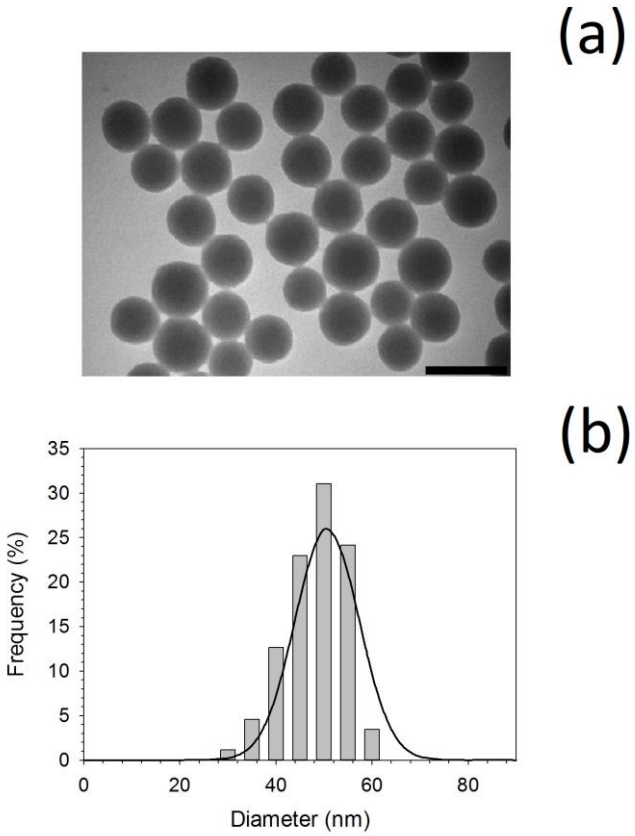

Figure 2. Example of TEM image of unfunctionalised silica nanoparticles (a). Bar equivalent to 100 nm. Size distribution of unfunctionalised silica nanoparticles (columns) and corresponding Gaussian distribution (solid line) (b).

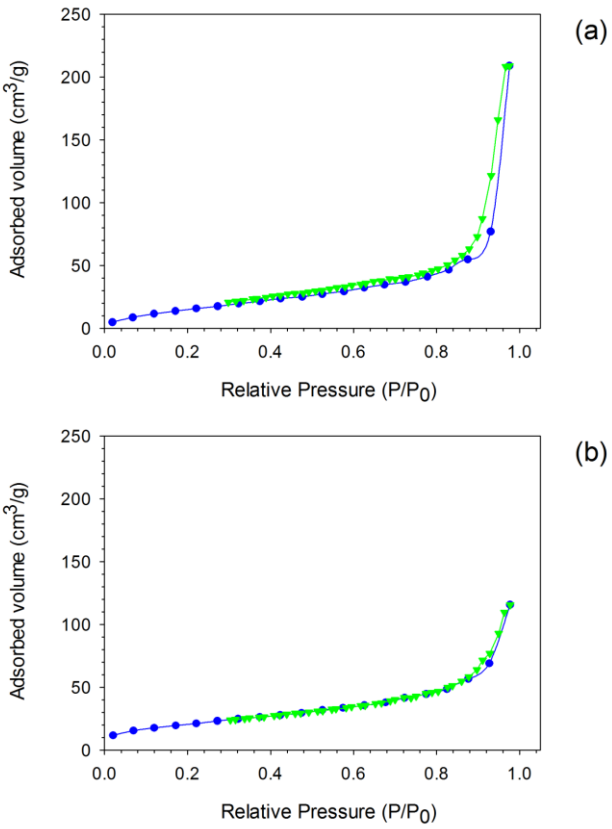

Figure 3. Examples of nitrogen adsorption−desorption isotherm profiles of (a) silica nanoparticles and (b) silica with entrapped gentamicin. Adsorption is presented in blue and desorption in green.

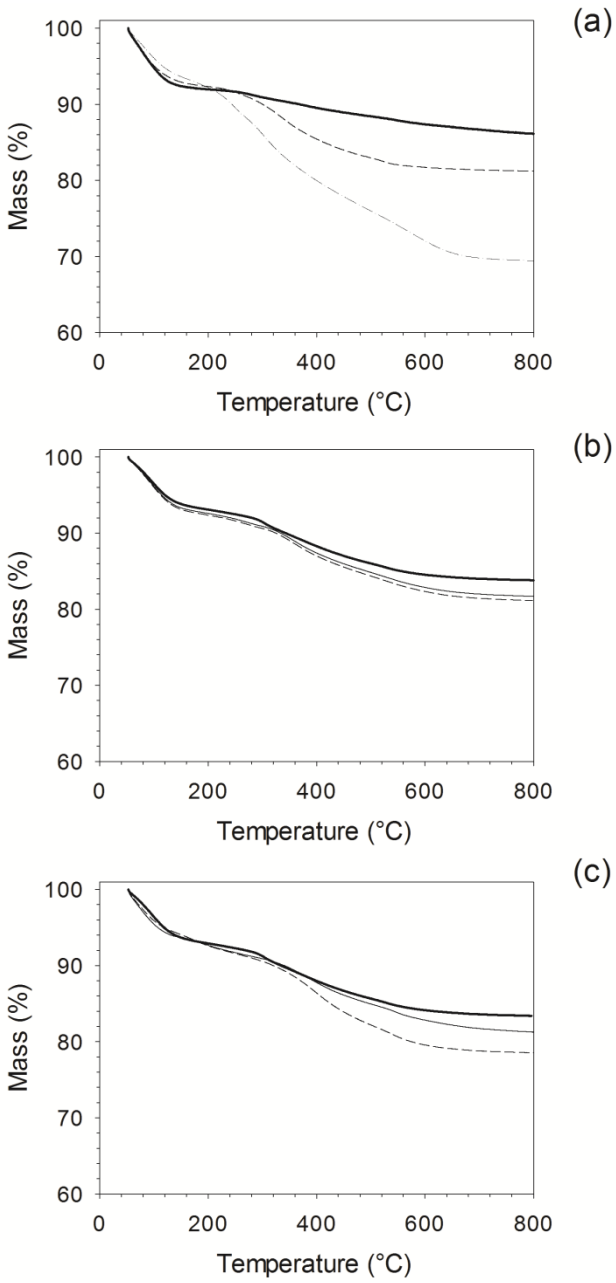

Figure 4. Thermal Gravimetric Analysis (TGA) of silica nanocarriers unfunctionalised (a), amino functionalised (b) and succinylated (c).

unload nanoparticles adsorbed gentamicin conjugated gentamicin

entrapped gentamicin

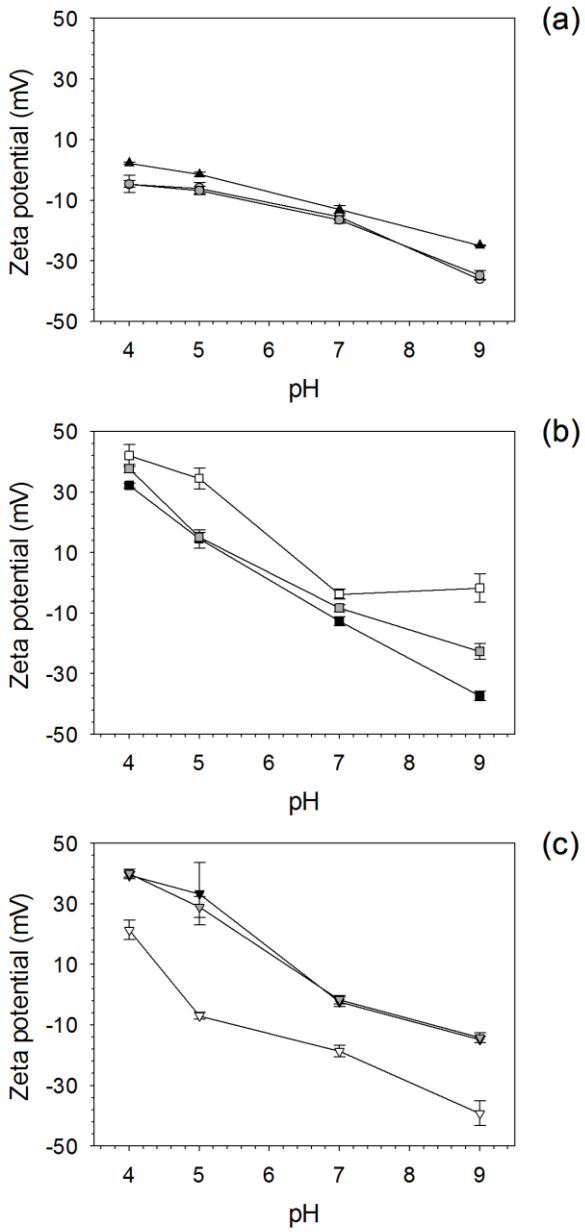

Figure 5. Zeta potential of silica nanocarriers unfunctionalised (a), amino functionalised (b) and succinylated (c).

unfunctionalised (○), amino functionalised (□) and carboxyl acid functionalised (▽). Symbols filled in black for nanocarriers with conjugated gentamicin; symbols filled in gray for nanocarriers with adsorbed gentamicin; nanocarriers with entrapped gentamicin (▲).

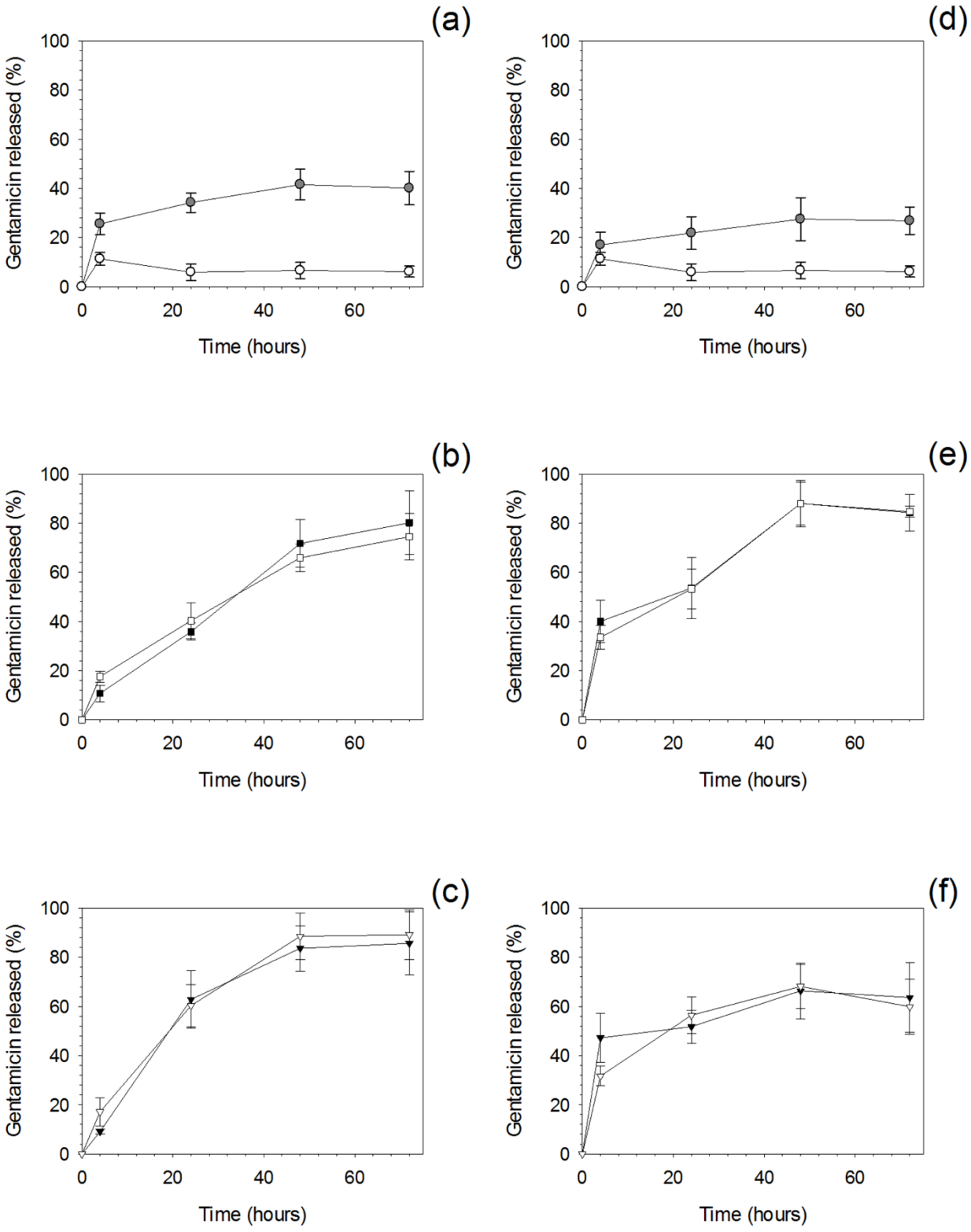

Figure 6. Cumulative release of gentamicin from silica nanocarriers at pH =5 (a, b, c) and pH =7.4 (d, e, f) for unfunctionalised (circles), amino functionalised (squares) and carboxyl acid functionalised (triangles). Symbols filled in black for nanocarriers with conjugated gentamicin; empty symbols for nanocarriers with adsorbed gentamicin; symbols filled in grey for nanocarriers with entrapped gentamicin.

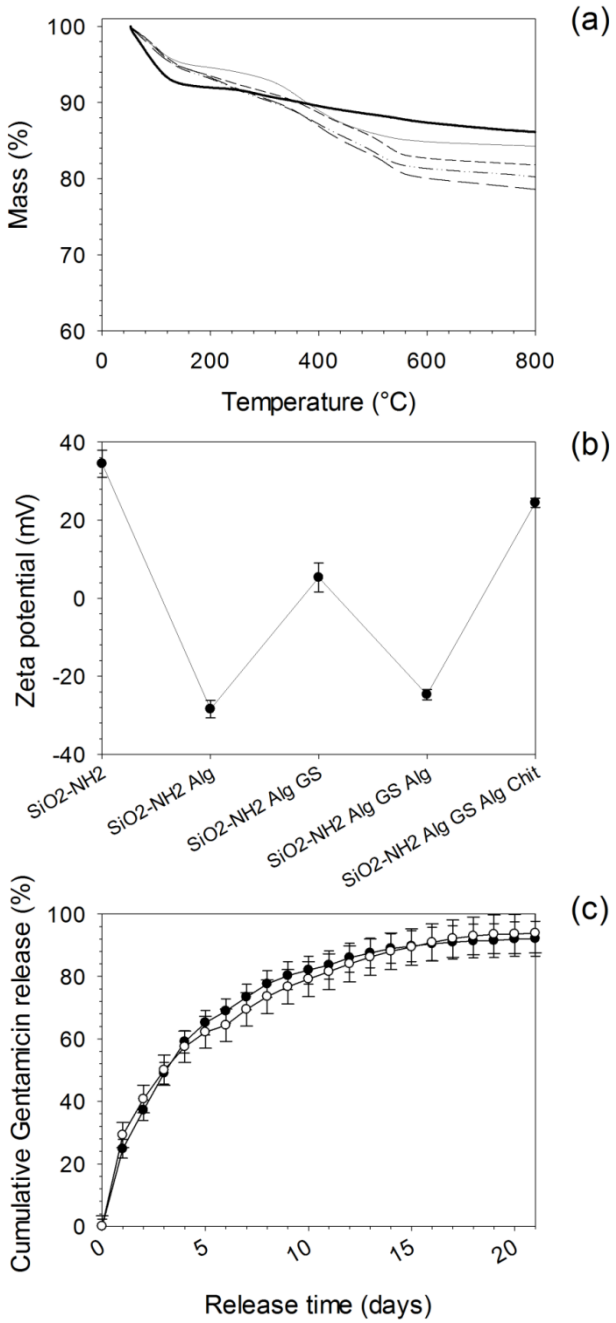

Figure 7. Thermal Gravimetric Analysis (TGA) (a) and zeta potential (b) of silica nanocarriers after each deposited layer during LbL coating. Cumulative release of gentamicin (c) from silica nanocarriers coated through LbL at pH = 5 (●) and pH = 7.4 (○)

SiO_2-NH_2 — SiO_2-NH_2 - Alg -------- SiO_2-NH_2 Alg - GS

SiO_2-NH_2 Alg - GS - Alg – – – – SiO_2-NH_2 - Alg - GS - Alg - Chit